電氣學會 論文誌 37卷 4號 1988年 4月

전류원 인버터로 구동되는 유도전동기의 맥동토오크

論 文
37~4~1

Steady-State Torque Pulsations in Current Source Inverter Fed Induction Motor Drives

愼 輝 範* · 尹 明 重**
(Hwi-Beom Shin · Myung-Joong Youn)

요 약

전류원 인버터로 구동되는 유도전동기의 수정된 등가회로의 벡터선도로부터 정상상태에서의 평균 토오크 및 맥동토오크를 쉽게 계산할 수 있는 간단한 방식이 제안된다. 또한, 이 방식으로 부터 토오크 맥동을 감소시키기 위한 펄스폭 변조 방식 및 직류 매개전류 변조 방식이 적용될 경우의 발생토오크를 계산할 수 있다. 제시된 방식의 타당성을 검증하기 위하여 유도 전동기의 D-Q방정식으로 부터 얻어진 컴퓨터 결과와 비교되어지며, 전류원으로 구동되는 유도전동기의 맥동 토오크는 전압원과는 다르게 부하조건에 따라 달라짐을 알 수 있다.

Abstract–A simple method that estimates the torque fluctuations in induction motor driven by CSI under steady state condition is presented and that uses the phasor diagram from the modified single-phase equivalent circuit. This method is also applied to evaluate the PWM and programmed dc link modulation techniques for reducing the torque pulsations. The simplified calculations are compared with the exact digital solutions from machine D-Q equation. It is noted that the torque pulsations in induction motor driven by CSI are dependent upon the load condition unlike VSI.

1. Introduction

Torque pulsations occur inherently over the entire operating range in induction machines driven by current source inverter(CSI). These torque pulsations are most apparent and troublesome at fundamental frequencies of zero to approximately five to ten percent of base frequency[1]. Therefore, an estimation of the amplitude of these torque pulsations under steady state will be useful in a prelimianry study of the current source inverter induction motor drive for a particular load. The machine D-Q model has been usuall used to calculate the torque pulsations with aid of computer[2) 3)]. This digital solutions include the inverse and exponential terms of matrices so that the hand calculations using this machine D-Q model are very difficult. When the current modulation techniques are adopted, especially, the torque fluctuations under steady-state condition cannot be easily calculated. The model normally used for studying the steady-state behavior of the machine is the single- phase equivalent circuit[4)].

In this paper, an easy method for evaluating the torque pulsations with nonsinusoidal applied current is described using the modified single-phase equivalent circuit of induction machine. Fig. 1 shows the schematic diagram for the CSI-induction motor. The three-phase rectangular wave currents, which flow for only 120 degrees of each half-cycle, are basically considered and this method is also applied to evaluate

* 正 會 員：韓國科學技術院 電氣 및 電子工學科 博士課程
** 正 會 員：韓國科學技術院 電氣 및 電子工學科 副教授 · 工博
接受日字：1987年12月11日
1次修正：1988年 3月29日

the PWM and programmed dc link current variation. The simplified calculations using the proposed method are compared with the digital solution of the exact D-Q machine equation under steady-state condition.

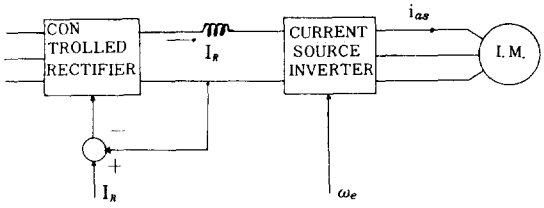

Fig. 1. Schematic diagram for CSI-induction motor.

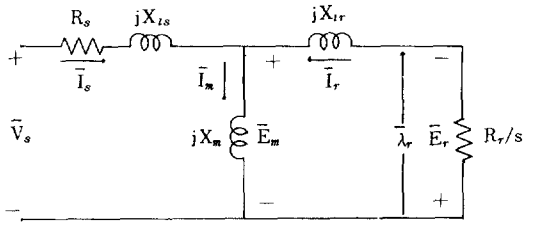

Fig. 2. Conventional equivalent circuit of induction motor.

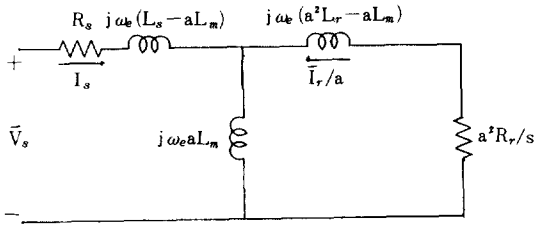

Fig. 3. Generalized equivalent circuit of induction motor.

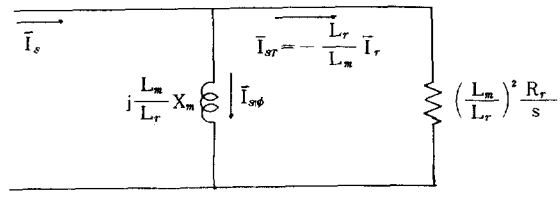

Fig. 4. Modified equivalent circuit of induction motor when driven by CSI.

2. Modified Single-Phase Equivalent Circuit

Torque pulsations of induction motor driven by voltage source inverter have been estimated using the conventional equivalent circuit shown in Fig. 2 [4]. Since the rotor branch in this equivalent circuit consists of the rotor leakage reactance and resistance, the expressions for the rotor current and internal voltage are very complex. Therefore, it is difficult to calculate the torque fluctuations of induction motor driven by CSI using this conventional circuit without aid of computer. Thus, it is necessary to modify this conventional circuit for estimating these torque fluctuations. Fig. 3 shows the generalized equivalent circuit of induction machine with an arbitrary referral ratio of 'a'[5]. A conventional circuit can be obtained from this generalized circuit by choosing 'a' to be the stator to rotor effective turns ratio. An extremely useful form of this circuit for calculating torque pulsations is obtained by choosing the referral ratio such that the series reactance in the rotor branch is zero. Setting this element equal to zero in the general circuit of Fig. 3 yields the value of the required referral ratio as

$$a=L_m/L_r \tag{1}$$

With this choice of 'a' the general circuit can be reduced to the one shown in Fig. 4. The stator branch can be excluded in this modified circuit because the induction motor is driven by CSI.

It is noted that the stator current is divided into two components ; one is through the new magnetizing branch expressed as $I_{s\phi}$ and another is through the new rotor resistance expressed as I_{sT}. These are the two components of stator current which produce the rotor flux and shaft torque, respectively.

The vlotage $\bar{E}_r$ is equal to the negative of the time rate of change of the rotor flux linkage $\bar{\lambda}_r$ from the conventional circuit shown in Fig. 2, as

$$\bar{E}_r=-j\omega_e\bar{\lambda}_r \tag{2}$$

From the citcuit shown in Fig. 4, the current $\bar{I}_{s\phi}$ is given by

$$\bar{I}_{s\phi}=\frac{\bar{E}_r}{j\omega_e L_m} \tag{3}$$

Combining (2) and (3) yields

$$\bar{\lambda}_r=L_m\cdot\bar{I}_{s\phi} \tag{4}$$

which clearly means that the rotor flux is produced by $\bar{I}_{s\phi}$

The torque component of stator current is given by

$$\bar{I}_{sT}=-\frac{L_r}{L_m}\bar{I}_r \tag{5}$$

Therefore, the stator current is

$$\bar{I}_s=I_{sT}+jI_{s\phi} \tag{6}$$

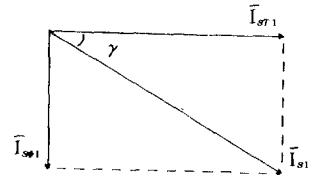

Fig. 5. Phasor diagram for fundamental component of stator current.

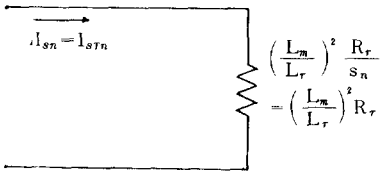

Fig. 6. Modified equivalent circuit for n th harmonic stator current.

The developed torque is represented in the conventional circuit as

$$T_e=\frac{3P}{2}\cdot\frac{E_r\cdot I_r}{\omega_e} \tag{7}$$

and this torque, however, can be expressed in the modified circuit using (2), (3), (5) and (7) as

$$T_e=K_t\cdot I_{s\phi}\cdot I_{sT} \tag{8}$$

where

$$K_t=\frac{3P}{2}\cdot\frac{L_m^2}{L_r} \tag{9}$$

Therefore, the amplitude of torque pulsations can be calculated from these two components of stator current.

Fig. 5. shows the phasor diagram for the fundamental component of stator current from (6) and the angle γ is given by

$$\cos\gamma=\frac{\omega_e L_r}{\sqrt{(\omega_e L_r)^2+(R_r/s)^2}} \tag{10}$$

For the n-th harmonic stator current, the following relations are satisfied.

$$s_n \simeq 1 \tag{11}$$

and

$$n\omega_e L_m >> (L_m/L_r)\cdot(R_r/s_n) \tag{12}$$

where s_n denotes the slip for the n-th harmonic component. These conditions are normally valid. Since the rotor flux produced by the harmonic current can be negligible, the modified equivalent circuit for the n-th harmonic current can be redrawn as shown in Fig. 6 and

$$I_{sTn}=I_{sn}\cdot \tag{13}$$

In the following calculations of torque pulsations, the harmonic torques due to the interactions of fundamental rotor flux and harmonic torque components of stator current are only considered because the rotor harmonic fluxes have small effects on the torque pulsations.

3. Torque Calculations Using Phasor Diagram

3.1 Quasi six-stepped current waveform

The motor line currents produced by CSI are shown in Fig. 7. If I_R is the magnitude of the current in the dc link, one phase stepped current can be represented using the Fourier series expansion as

$$i_{as}(\omega_e t)=\sqrt{2}\,(I_{s1}\sin\omega_e t+I_{s5}\sin 5\omega_e t+I_{s7}\sin 7\omega_e t+ I_{s11}\sin 11\omega_e t+I_{s13}\sin 13\omega_e t+\cdots) \tag{14}$$

where

$I_{s1}=(\sqrt{6}/\pi)I_R$, $I_{s5}=-I_{s1}/5$
$I_{s7}=-I_{s1}/7$, $I_{s11}=I_{s1}/11$,
$I_{s13}=I_{s1}/13$, ……,

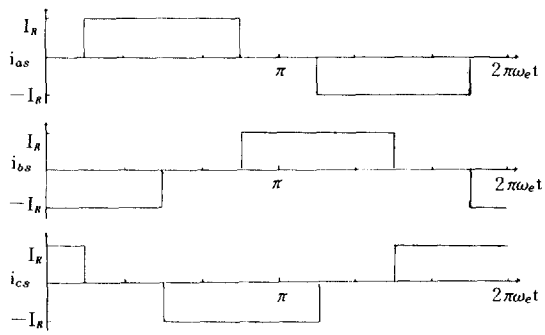

Fig. 7. Quasi six-stepped current waveforms.

In a three-phase machine, Fig. 8(a) shows all five of these current phasors in a single diagram, rotating at their own synchronous speeds and directions. For simplicity, Fig. 8(b) is obtained by giving the whole diagram a clockwise rotation with the speed of ω_e to make the fundamental phasor stationary. Fig. 8 (b) shows the sixth-and twelfth-harmonics due to $I_{s\phi 1}$ with I_{s5} and I_{s7}, and $I_{s\phi 1}$ with I_{s11} and I_{s13}, respectively. From this diagram, an average torque and harmonic torques can be obtained as

$$T_{e1}=K_t\cdot I_{s\phi 1}\cdot I_{sT1}=K_t\cdot I_{s\phi 1}\cdot I_{s1}\cdot\cos\gamma \tag{15}$$

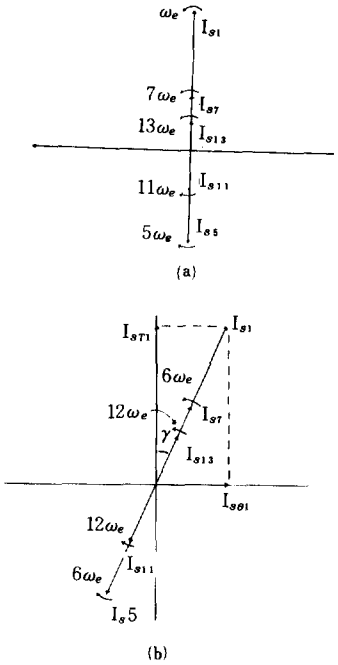

Fig. 8. Phasor diagram for fundamental and harmonic currents.

$$T_{e6}=K_t \cdot I_{s\phi 1} \cdot [(I_{s7}-I_{s5}) \cos\gamma \cos 6\omega_e t + (I_{s7}+I_{s5}) \sin\gamma \sin 6\omega_e t \ ] \quad (16)$$

$$T_{e12}=K_t \cdot I_{s\phi 1} \cdot [(I_{s13}-I_{s11}) \cos\gamma \cos 12\omega_e t + (I_{s13}+I_{s11} \sin\gamma \sin 12\omega_e t \ ] \quad (17)$$

where

$$I_{s\phi 1}=I_{s1} \cdot \sin\gamma. \quad (18)$$

Hence, the torque pulsations in CSI fed induction motor drive are dependent upon the load condition unlike these in VSI fed induction motor drive. The maximum torque $T_{e,\,max}$ is obtained from (15) and (18) as

$$T_{e,\,max}=(K_t/2) \cdot I^2_{s1} \quad (19)$$

when slip s_{max} is

$$s_{max}=R_r / \omega_e L_r \quad (20)$$

where

$$L_r=L_m+L_{lr} \quad (21)$$

In reality, the stator core is saturated at near or above s_{max}. Thus, $T_{e,\,max}$ and s_{max} are calculated from (19) and (20) with the saturated magnetizing inductance. Also, this maximum torque is affected by the voltage capability of CSI. However, the slip relation given by (20) insures the operating ranges of CSI fed induction motor drives.

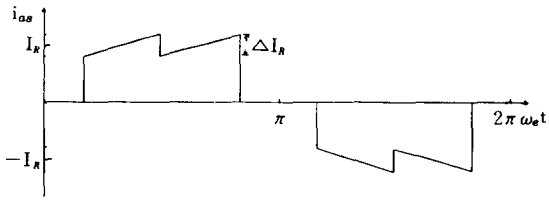

Fig. 9. DC link current having the sawtooth shape.

3.2 DC link current modulation

When the dc-link current is modulated in order to reduce the torque fluctations, the shape of dc-link current can be approximately considered as the sawtooth shape shown in Fig.9. This link current can be written using the Fourier series expansion as

$$i_{as}(\omega_e t)=\sum_{n=1}^{\infty} \frac{4}{n\pi} \cdot \sin\frac{n\pi}{2} \cos(n\pi) \left[\left(-\sin\frac{n\pi}{2}\right) \cdot I_R \sin(n\omega_e t)+\left(\frac{3}{n\pi}\sin\frac{n\pi}{3} -\cos^2\frac{n\pi}{6}\right) \cdot \triangle I_R \cos(n\omega_e t) \right]$$

$$= \sqrt{2} \cdot [(I_{s1} \sin\omega_e t+I_{s5} \sin 5\omega_e t+I_{s7} \sin 7\omega_e t+ I_{s11} \cdot \sin 11\omega_e t+\cdots)+(\triangle I_{s1} \cos\omega_e t+\triangle I_{s5} \cos 5\omega_e t +\triangle I_{s7} \cos 7\omega_e t+\triangle I_{s11} \cos 11\omega_e t+\cdots)] \quad (22)$$

where

$$\triangle I_{s1}=-\frac{\sqrt{6}}{\pi}\left(\frac{3}{\pi}-\frac{\sqrt{3}}{2}\right)\triangle I_R, \triangle I_{s5}=\frac{\sqrt{6}}{5\pi}\left(\frac{3}{5\pi}+\frac{\sqrt{3}}{2}\right)\triangle I_R,$$

$$\triangle I_{s7}=\frac{\sqrt{6}}{7\pi}\left(\frac{3}{7\pi}-\frac{\sqrt{3}}{2}\right)\triangle I_R, \triangle I_{s11}=-\frac{6}{11\pi}\left(\frac{3}{11\pi}+\frac{\sqrt{3}}{2}\right)\triangle I_R$$

$$\triangle I_{s13}=-\frac{\sqrt{6}}{13\pi}\left(\frac{3}{13\pi}-\frac{\sqrt{3}}{2}\right)\triangle I_R, \cdots$$

In (22), it is noted that one phase modulated current is divided into two compoments due to the average link current I_R and the deviated link current $\triangle I_R$

The related current phasor diagram is shown in Fig. 10. From this diagram, the torque pulsations are calculated as

$$T_{e1}=K_t \cdot I_{s\phi 1} \cdot (I_{s1} \cdot \cos\gamma+\triangle I_{s1} \sin\gamma) \quad (23)$$

$$T_{e6}=K_t \cdot I_{s\phi 1}\{ [(I_{s7}-I_{s5}) \cos\gamma+$$

$$(\triangle I_{s5}+\triangle I_{s7})\sin\gamma]\cos 6\omega_e t\ \}+\ [(I_{s7}+I_{s5})\sin\gamma+(\triangle I_{s5}-\triangle I_{s7})\cos\gamma]\ \sin 6\omega_e t\ \} \quad (24)$$

$$T_{e12}=K_t\cdot I_{s\phi 1}\{\ [(I_{s13}-I_{s11})\cos\gamma+(\triangle I_{s11}+\triangle I_{s13})\sin\gamma\ ]\cos 12\omega_e t+[(I_{s13}+I_{s11})\sin\gamma+(\triangle I_{s11}-\triangle I_{s13})\cos\gamma]\sin 12\omega_e t\} \quad (25)$$

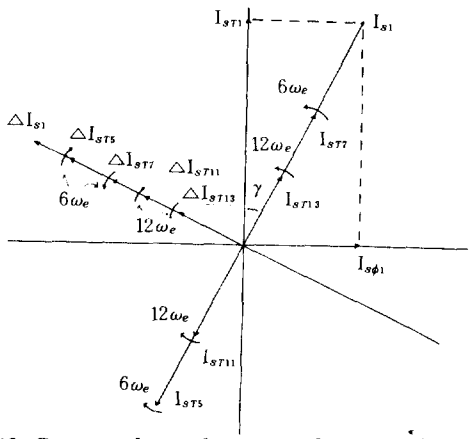

Fig. 10. Current phasor for sawtooth-type link current.

The six-stepped current contains only sine terms as in (14), but the stator current contains both sine and cosine, namely 90°-phase different, terms in case of the programmed dc link modulation. Hence, this modulation reduces the torque pulsations as the magnitude of sine terms in harmonic torques given by (24) and (25) is reduced.

3.3 PWM current modulation

The objective of PWM current modulation is to eliminate the lowest motor current harmonics and consequently eliminate the lowest torque harmonics. To obtain the identical three-phase output currents from CSI, the current pulse pattern must have the following characteristics[1] :

i) The pulse pattern should be quarter-wave and half-wave symmetric.

ii) No PWM is permitted between 60° to 120° portion of the half-cycle.

iii) For 30° on either side of the 30° and 150° portions, the pulse pattern must be an inverse mirror image.

Fig. 11 shows the general PWM pattern for 5 and 7 pulses per half-cycle. Because these PWM waveforms are half-and quater-wave symmetric, one phase curr, ent for p-pulse can be expressed as

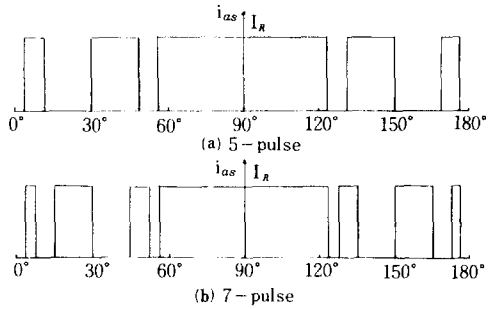

Fig. 11. General patterns for 5 and 7 pulses per half-cycle PWM.

$$i_{as}(\omega_e t)=\sum_{n=1,5,7}\frac{4}{n\pi}I_R[\sum_{k=1}^{p}(-1)^{k+1}\cos(n\alpha_k)]\sin(n\omega_e t) \quad (26)$$

In (26), the magnitudes of harmonic currents in six-stepped waveform of (14) are only changed. Thus, the torque pulsations can be estimated by the same phasor diagram of the quasi six-stepped current waveform. This PWM method reduces the lowest torque harmonics by reducing the lowest harmonic currents.

4. Comparison of Simplified and Exact Calculation

Simplified torque calculations from phasor diagram are compared with the computed results obtained by digital solutions of the machine D-Q equation[2][3]. The followings are the machine parameters obtained from a 25hp, 4-pole 230V 64A three-phase 60HZ machine :

R_s=0.0380 pu ; R_r=0.0197 pu

X_s=2.77 pu ; X_r=2.89 pu

X_m=2.68 pu.

Table I shows the average and harmonic torques under several different operating conditions when the applied stator currents are six-stepped waveforms. The simplified calculations are nearly equal to the exact solutions. The result shows that the magnitude of torque pulsation decreases as the slip increases. Thus, it can be seen that torque pulsations increase as the load increases under the normal operation of CSI induction motor drives. This fact can be acknowledged from (16) and (17) using the trigonomet-

Table I. Torque comparisons with six stepped-waveform.

ω_e	ω_m	I_R	Average Torque[pu]		6th harmonic[pu]		12th harmonic[pu]	
[Hz]	[rpm]	[A]	Simplified	Exact	Simplified	Exact	Simplified	Exact
60	1770	82	1.087	1.090	0.150	0.147	0.0686	0.0671
60	1720	82	0.496	0.497	0.038	0.036	0.0143	0.0136
60	1670	82	0.317	0.317	0.021	0.019	0.0067	0.0062
30	860	82	0.930	0.933	0.110	0.101	0.0489	0.0476
30	810	82	0.458	0.458	0.034	0.031	0.0124	0.0116
5	125	82	1.301	1.305	0.224	0.216	0.1050	0.1030
5	115	82	1.039	1.042	0.137	0.133	0.0620	0.0610
5	105	82	0.847	0.859	0.094	0.091	0.0411	0.0399

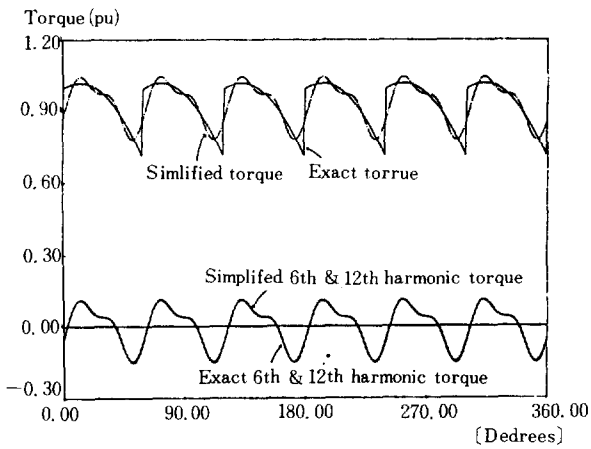

Fig. 12. Torque pulsations in induction motor with quasi six-stepped currents : ω_e=30[HZ], ω_{sl}=1. 34[HZ], I_R=82[A].

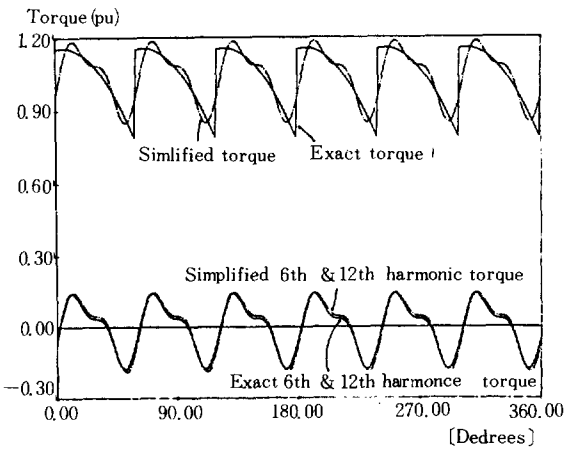

Fig. 13. Torque pulasations in induction motor with quasi six-stepped currents : ω_e=5[HZ], ω_{sl}=1. 2[HZ], I_R=82[A].

ric relations. Fig. 12 and Fig. 13 show the torque pulsations when the six-stepped currents are applied to induction motor. The simplified 6th and 12th harmonic torques resemble the exact ones but the simplified calculations are erroneous when the percent slip increases. However, this calculations are very useful in normal slip operation. The simplified torque with only 6th and 12th harmonics is close to the torque with all harmonics obtained from machine D-Q equation, although the harmonic torques due to harmonic rotor fluxes are neglected.

Whan the dc link current is modulated to the sawtooth waveforms, the relevant harmonic torques are shown in Table II under several different operation conditions. It can be seen that there is a certain deviated current to minimize the harmonic torques and the reduction of torque pulsations is dependent upon the deviated link current. The average torque is not nearly varied by this link modulation. Fig. 14 shows the lowest possible torque pulsation. However, Fig. 15 shows the torque pulsation when under-modulated so that the link current needs to be more deeply modulated in order to reduce it. The simplified calculations can be seen to be close to the exact ones.

Table II. Torque comparisons with sawtooth-type waveform (I_R=82[A]).

ω_e	ω_m	ΔI_R	Average Torque[pu]		6th harmonic[pu]		12th harmonic[pu]	
[Hz]	[rpm]	[%]	Simplified	Exact	Simplified	Exact	Simplified	Exact
30	860	10	0.930	0.931	0.0701	0.0634	0.0244	0.0266
30	860	15	0.930	0.931	0.0627	0.0592	0.0163	0.0144
30	860	20	0.930	0.931	0.0682	0.0716	0.0177	0.0216
5	115	10	1.039	1.039	0.0884	0.0714	0.0338	0.0284
5	115	15	1.039	1.039	0.0754	0.0569	0.0244	0.0158
5	115	25	1.039	1.038	0.0885	0.0861	0.0252	0.0306

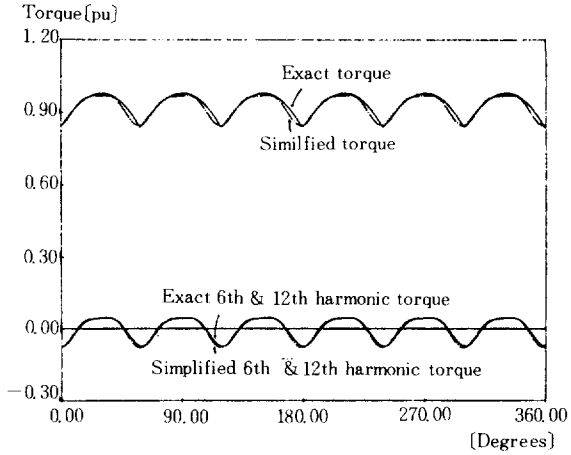

Fig. 14. Torque pulsations in induction motor with sawtooth type link current : ω_e=30[HZ], ω_{sl}=1. 34[HZ], I_R=82[A], $\triangle I_R$=15[%].

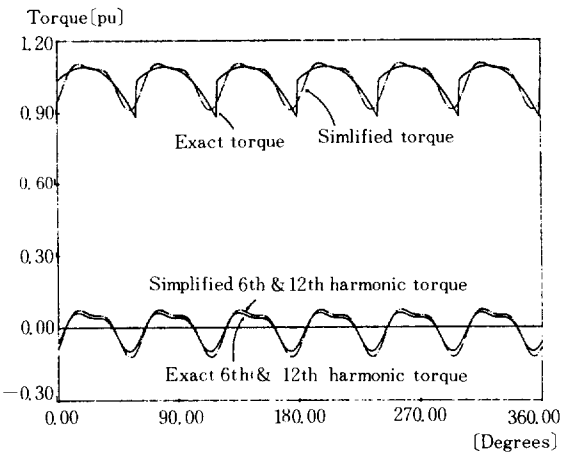

Fig. 15. Torque pulsations in induction motor with sawtooth type link current :ω_e=5[HZ], ω_{sl}=1. 2[HZ], I_R=82[HZ], $\triangle I_R$=10[%].

5. Conclusion

A simple method of estimating torque fluctuations of CSI induction motor drives under steady state, using the phasor diagram from the modified single-phase equivalent circuit, has been presented. The proposed method has the following advavtages ;

i) The developed torque can be calculated without aid of computer.

ii) The torque fluctuations are easily calculated for PWM and programmed dc link current variation techniques.

iii) Torque characteristics can be easily investigated in preliminary study.

The result shows that the PWM method reduces the torque pulsation by reducing the lowest harmonic currents itself and the programmed dc link current modulation reduces these by adding the 90°-phase different current to the six-stepped stator current. Also, it can be seen that the torque pulsations in induction motor driven by CSI are dependent upon the load condition unlike the voltage source inverter.

REFERENCES

1) J. Zubek, "Evaluation of Techniques for Reducing Shaft Cogging in Current Fed AC Drives," IEEE-IAS Annual Meeting Conference Record, 1978.

2) T. A. Lipo and E. P. Cornell, "State-Variable Steady- State Analysis of a Controlled Current Induction Motor Drive," IEEE Trans. Ind. Appl., vol. IA-11, pp. 704-712, Nov. / Dec. 1975.
3) G. K. Creighton, "Current-source invertor-fed induction motor torque pulsations," IEE PROC. vol. 127, No. 4, JULY 1980.
4) S. D. T. Robertson and K. M. Hebbar, "Torque Pulsations in Induction Motors with Inverter Drives," IEEE Trans. Ind. Gen. Appl., vol. IGA-7, pp. 318-323, Mar. / Apr. 1971.
5) D. W. Novotny and R. D. Lorenz, "Introduction to Field Orientation and High Performance AC Drives," IEEE IAS Tutorial Course, 1986.